Matrix-isolation and ab initio study of the complex between formic acid and xenon

ARTICLE *in* JOURNAL OF MOLECULAR STRUCTURE · APRIL 2012

Impact Factor: 1.6 · DOI: 10.1016/j.molstruc.2012.05.027

Journal of Molecular Structure 1025 (2012) 132–139

Contents lists available at SciVerse ScienceDirect

Journal of Molecular Structure

journal homepage: www.elsevier.com/locate/molstruc

Matrix-isolation and ab initio study of the complex between formic acid and xenon

Qian Cao [a], Mia Melavuori [a], Jan Lundell [b], Markku Räsänen [a], Leonid Khriachtchev [a,*]

[a] Department of Chemistry, University of Helsinki, P.O. Box 55, FI-00014 Helsinki, Finland
[b] Department of Chemistry, University of Jyväskylä, P.O. Box 35, FI-40014 Jyväskylä, Finland

HIGHLIGHTS

- Four *trans*-FA···Xe and four *cis*-FA···Xe complexes are predicted theoretically.
- Two *trans*-FA···Xe and two *cis*-FA···Xe complexes are found experimentally.
- Stabilization of *cis*-FA is observed in the H-bonded complex.
- Destabilization of *cis*-FA is observed in the non-H-bonded complex.

ARTICLE INFO

Article history:
Available online 16 May 2012

Keywords:
Formic acid
Xenon
Hydrogen bond
Ab initio
Tunnelling
Matrix isolation

ABSTRACT

We report on the identification of the complexes of formic acid (FA) and Xe in an argon matrix. The geometries, interaction energies, reaction barriers, and vibrational spectra of the FA···Xe complexes are calculated at the MP2 level of theory. The calculations reveal four structures for the *trans*-FA···Xe complex and four structures for the *cis*-FA···Xe complex. In the experiments, two structures of the *trans*-FA···Xe complex are observed after deposition of FA/Xe/Ar matrices, with and without OH···Xe interaction (H-bonded and non-H-bonded structures). The *cis*-FA···Xe complex was synthesized by vibrational excitation of the non-H-bonded *trans*-FA···Xe complex. The non-H-bonded and H-bonded structures of the *cis*-FA···Xe complex are observed after the excitation. The decay of the H-bonded and non-H-bonded *cis*-FA···Xe complexes in an argon matrix is, respectively, substantially slower and faster compared to the *cis*-FA monomer. This observation is explained by the different tunnelling barriers for these species.

1. Introduction

Formic acid (HCOOH, FA) is a useful model compound for understanding the properties of more complicated molecules, in particular, of biological interest. As the simplest organic acid, FA exhibits the conformational isomerism with respect to the rotation about the single C—O bond, which is a typical phenomenon in the conformational processes in carboxylic acids. Two conformers (cis and trans) of FA exist, which differ by the orientation of the OH group. The cis form of FA is higher in energy than the trans form by approximately 1365 cm^{-1} (gas-phase experimental data) [1], and the calculated trans-to-cis conversion barrier is 44 kJ mol^{-1} (3921 cm^{-1}) [2]. Recently, extensive studies have been carried out on FA in low-temperature matrices, particularly focusing on the trans–cis conformational interconversion [3]. The *cis*-FA conformer can be prepared by vibrational excitation of the trans form by IR light, and it decays back to *trans*-FA in the dark via tunnelling of the H atom through the torsional barrier. The tunnelling rates are strongly dependent on the matrix material, changing with the matrix as $k_{Ne} > k_{Ar} > k_{Kr} > k_{Xe}$ [3,4]. Detailed infrared (IR) spectroscopic studies on the trans and cis conformers of FA have been reported in different matrices [5–10]. Similar conformational processes have also been found for acetic acid (CH_3COOH) [10–12] and propionic acid (CH_3CH_2COOH) [13].

FA is also an important model to study non-covalent interactions. There have been many experimental studies of *trans*-FA and *cis*-FA complexes, trans–trans, trans–cis, and cis–cis dimers in rare-gas matrices [14–21]. Light-induced conformational change has allowed preparing dimers and complexes of the higher-energy conformer. It has been shown that the *cis*-FA conformer can be stabilized by the intermolecular interactions. For example, the lifetime of the *cis*-FA···N_2 complex in an argon matrix is *ca.* 6.5 times longer than that of the *cis*-FA monomer [15]. A recent study on two trans–cis dimers (named tc1 and tc4) has shown that the stability of these two dimers against hydrogen tunnelling is improved compared to the *cis*-FA monomer [18,19]. In these dimers, the tunnelling H atom of *cis*-FA is "free". When the OH hydrogen of the cis conformer is involved in hydrogen bonding, the trans–cis dimers (tc2, tc3, and tc5) are practically stable at low temperatures [20]. Similar stabilization

* Corresponding author.
E-mail address: leonid.khriachtchev@helsinki.fi (L. Khriachtchev).

0022-2860/$ - see front matter © 2012 Elsevier B.V. All rights reserved.
http://dx.doi.org/10.1016/j.molstruc.2012.05.027

effects have also been found for the intermolecular OH···O bonding, which stabilizes *cis*-FA upon interaction with a water molecule or an oxygen atom so that the hydrogen tunnelling is completely suppressed at low temperatures [16,17].

Since rare-gas matrices are widely used to study conformational changes [22], understanding of the interactions between rare-gas atoms and different conformers is important. The 1:1 *trans*-FA···Ar complex was firstly studied by Ioannou and Kuczkowski in their microwave experiments [23], and the obtained complex was a planar structure with an argon atom positioned at distances of 3.71 and 2.81 Å from the carbonyl oxygen and acidic hydrogen, respectively. Several structures of the *trans*- and *cis*-FA···Ar complexes have been found in calculations [24,25]. The most stable structure has the argon atom interacting with the OH group of FA, and the calculated geometry agrees with the experimental data [23]. Similar structures were predicted for the *trans*- and *cis*-FA···Kr complexes [26].

In the present work, we study the complexes of *trans*- and *cis*-FA with a Xe atom using IR spectroscopy in an argon matrix. The identification of the 1:1 FA···Xe complexes is aided by ab initio calculations. The decay of the *cis*-FA···Xe complexes is measured and discussed. This work is partially motivated by anaesthetic properties of xenon [27], which enhances the importance of research on the interaction between Xe atoms and organic molecules.

2. Computational details and results

2.1. Computational details

The calculations were performed using Gaussian 09 package [28]. The aug-cc-pVDZ basis set was used for the atoms of FA and the aug-cc-pVDZ-PP basis set enabling the Stuttgart effective core potential was used for Xe [29]. The equilibrium geometries, interaction energies, reaction barriers, and vibrational frequencies of the *trans*- and *cis*-FA monomers and the complexes with Xe were calculated using the second order Møller-Plesset perturbation theory (MP2). Optimizations were performed by using the Opt = Tight criteria, and BSSE post-correction was applied for computed interaction energies. The spectral shifts for the complexes were calculated as the difference between the complex and monomer vibrational frequencies. This computational method was used for the calculations of the FA···Ar and FA···Kr complexes [24–26]. Most of the transition state geometries were optimized freezing Xe and C atoms for the various local minimum structures to obtain energy contributions with respect to rotation of the —OH tail of FA. For structure **I** of the *cis*-FA···Xe complex, the Xe and O atoms were frozen during transition state optimization. All obtained transition states have only one imaginary frequency.

2.2. Computational results

Four local minima are found for both *trans*- and *cis*-FA···Xe complexes (see Fig. 1) These structures are similar to those obtained earlier for the FA···Ar and FA···Kr complexes [24–26]. For both *trans*- and *cis*-FA, structures **II**, **III** and **IV** are planar. Structure **I** is non-planar with the Xe atom above the FA molecule, the distance between the Xe and C atoms being 3.739 and 3.718 Å for the *trans*- and *cis*-FA···Xe complexes, respectively. In structure **II**, the Xe atom is bonded to the H atom of the OH group, while in structure **III** the Xe atom is interacting with the O atom of the carbonyl group. In structure **IV**, the Xe atom is attached to the H atom of the CH group, being heavily tilted towards the vicinal carbonyl group. The shortest intermolecular distances are found in structure **II**, where the Xe—H distances are 2.873 and 2.918 Å for the *trans*- and *cis*-FA complexes, respectively. The FA molecules in the complexes are structurally similar to the monomers, which is typical for weak intermolecular interactions. The CCSD(T) computations with the basis set used in the current study are in qualitative agreement with the presented MP2 results, and bring no new insight into the assignments. The biggest effect of using the CCSD(T) level of theory is a slight shortening of the intermolecular distance, which produces only small changes in the spectral shifts.

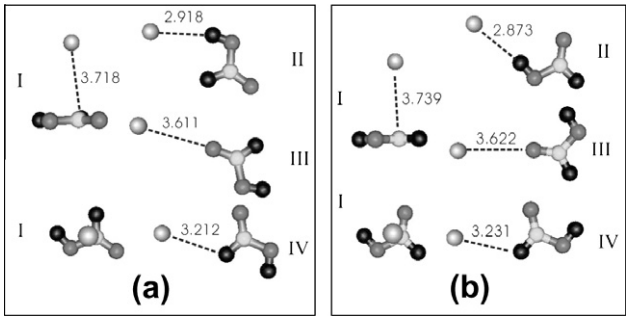

Fig. 1. Calculated structures of the *cis*-FA···Xe (a) and *trans*-FA···Xe (b) complexes. The distances are in angstroms.

The BSSE-corrected interaction energies are shown in Table 1. Complex **II** with an OH···Xe intermolecular bond is the most stable structure with CCSD(T)//MP2 interaction energies of −1.5 kJ mol^{-1} for *trans*-FA and −2.2 kJ mol^{-1} for *cis*-FA. The FA···Xe interaction energies are similar to those of the FA···Kr complexes [26] and somewhat bigger than those of the FA···Ar complexes [25].

The calculated vibrational spectra of the FA···Xe complexes are shown in Table 2. Structure **II** has the largest frequency shifts for both FA conformers. The OH stretching (νOH) mode of structure **II** is red-shifted by −26.9 cm^{-1} (*trans*-FA) and −22.8 cm^{-1} (*cis*-FA), and the absorption intensity grows from 73 to 241 km mol^{-1} for the *trans*-FA···Xe complex and from 73 to 182 km mol^{-1} for the *cis*-FA···Xe complex. For the *cis*-FA···Xe complex, large frequency shifts are predicted for the OCO bending (δOCO) (+35.6 cm^{-1}) and CO—COH deformation (+12.1 cm^{-1}) modes. For the *trans*-FA···Xe complex, a large shift is obtained for the torsional (τCOH) mode (+25.4 cm^{-1}). For structures **I**, **III** and **IV,** the spectral changes are relatively small. For the *cis*-FA···Xe complex, the largest frequency shift is found for the CH stretching (νCH) mode (+5.9, +6.1 and +8.3 cm^{-1} in structures **I**, **III** and **IV**, respectively). For the *trans*-FA···Xe complex, the interaction with Xe affects most the OH wagging (ωOH) mode in structures **I** (−3.6 cm^{-1}) and **IV** (+3.6 cm^{-1}), while in structure **III**, the largest shift is seen for the C=O stretching (νC=O) mode (−2.6 cm^{-1}).

Table 3 presents the stabilization barriers calculated for the *cis*-FA···Xe complexes. The highest barrier is obtained for the H-bonded structure **II**. Structure **I** has the smallest stabilization

Table 1
Calculated interaction energies (in kJ mol^{-1}) for the *cis*- and *trans*-FA···Xe complexes.[a]

Structure	MP2//MP2	CCSD(T)//MP2
cis-FA···Xe		
I	−1.7	−1.2
II	−2.4	−2.2
III	−1.5	−1.1
IV	−1.5	−1.2
trans-FA···Xe		
I	−1.5	−0.9
II	−1.7	−1.5
III	−1.4	−1.2
IV	−1.2	−1.0

[a] The aug-cc-pVDZ-PP basis set is used in all calculations.

Table 2
Calculated vibrational frequencies (in cm^{-1}) and infrared intensities (in km mol^{-1}) of the FA monomers and FA···Xe complexes.

Assignment[a]	Monomer		I		II		III		IV	
	Freq.	Intens.	Freq.	Intens.	Freq.	Intens.	Freq.	Intens.	Freq.	Intens.
cis-FA										
νOH	3792.8	73.2	3790.1	68.4	3770.0	181.9	3790.4	78.8	3792.0	75.1
νCH	3052.4	63.2	3058.3	53.8	3058.8	65.5	3058.5	65.7	3060.7	57.7
νC═O	1809.3	267.8	1807.8	232.4	1804.9	321.2	1805.4	305.5	1807.4	238.2
γCH	1408.0	0.1	1407.5	0.1	1406.9	1.2	1406.4	0.0	1406.8	2.2
CO—COH def	1274.4	294.0	1275.9	268.3	1286.5	222.3	1276.0	306.1	1274.7	332.2
COH—CO def	1098.2	67.2	1100.0	55.2	1106.2	80.6	1102.2	65.3	1101.4	82.6
ωOH	1022.7	0.3	1018.8	0.1	1026.0	0.1	1021.9	0.3	1024.5	0.1
τCOH	643.2	10.8	643.6	9.4	646.1	6.1	644.6	11.6	643.7	9.4
δOCO	523.7	83.3	518.8	97.4	559.3	54.4	526.7	82.7	526.2	81.3
Inter-			72.0	49.6	67.2	45.6	39.8	1.5	54.0	7.0
Molecular			38.9	0.4	65.0	5.3	32.4	53.2	47.4	35.8
Modes			25.7	26.2	29.9	5.6	8.4	9.6	35.0	9.5
trans-FA										
νOH	3728.6	72.6	3726.3	69.9	3701.7	241.2	3727.5	68.9	3727.4	77.3
νCH	3142.4	33.3	3140.9	27.6	3138.7	43.6	3142.6	34.2	3145.4	31.6
νC═O	1774.7	329.9	1774.1	287.0	1772.7	288.3	1772.1	378.2	1773.1	301.7
γCH	1398.2	1.2	1397.3	1.3	1399.1	3.8	1397.9	1.4	1397.4	1.3
CO—COH def	1296.3	8.4	1296.1	6.0	1302.3	12.0	1296.0	8.9	1296.3	10.9
COH—CO def	1118.4	269.6	1118.2	240.5	1122.5	255.6	1119.5	279.9	1118.6	311.9
ωOH	1047.9	4.4	1044.3	3.1	1049.8	3.4	1048.7	4.2	1051.5	3.3
τCOH	675.0	134.8	673.2	160.1	700.3	88.3	676.2	129.3	675.8	128.6
δOCO	619.2	38.8	619.2	35.4	622.3	39.2	619.6	39.2	619.5	46.0
Inter-			48.6	0.1	75.9	1.8	38.0	0.3	53.63	1.2
Molecular			38.9	1.4	65.6	2.9	13.9	1.1	45.8	0.1
Modes			25.7	1.4	18.9	1.4	9.9	1.2	34.1	2.1

[a] ν – stretching, ω – wagging, τ – torsion, δ – bending, def. – deformation. Assignment of the vibrational modes follows Ref. [35].

Table 3
Calculated stabilization barriers (in cm^{-1}, 1 kJ mol^{-1} = 83.6 cm^{-1}) for the *cis*-FA monomer and *cis*-FA···Xe complexes.[a]

Species	Barrier	ZPE-corrected
Monomer	3071	2698
I	2986[b]	2625[b]
	3072[c]	2711[c]
II	3281	2861
III	3094	2750
IV	3101	2745

[a] MP2/aug-cc-pVDZ-PP level of theory.
[b] Towards Xe.
[c] Away from Xe.

barrier if the H atom moves towards the Xe atom. Remarkably, this barrier is smaller than that of the *cis*-FA monomer. The stabilization barriers for structure **III** and **IV** are a little larger than that of the monomer.

3. Experimental details and results

3.1. Experimental details

The gaseous samples were prepared by mixing formic acid (HCOOH, Kebo Lab, 99%) with xenon and argon (AGA, 99.9999%). The matrices were deposited onto a CsI substrate typically kept at 12 K in a closed-cycle helium cryostat (Sumitomo Heavy Industries). The IR absorption spectra in the 4000–600 cm^{-1} spectral range were measured at 4.3 K with a Bruker VERTEX 80 FTIR spectrometer using resolution 0.25 or 0.5 cm^{-1} and co-adding 200 interferograms. Conformational changes were promoted by an optical parametric oscillator (OPO Sunlite, Continuum with an IR extension) providing tunable IR light with a pulse duration of 5 ns, linewidth of 0.1 cm^{-1}, and repetition rate of 10 Hz. A Burleigh WA-4500 wavemeter measured the OPO signal frequency, providing an absolute accuracy better than 1 cm^{-1} for the IR light. During the kinetic measurements, a long-pass filter transmitting below 1835 cm^{-1} was installed between the Globar source and the cryostat to eliminate broadband light-induced conformational conversion. The tunnelling decay was monitored by integrating the intensity of the COH—CO deformation bands.

3.2. trans-FA···Xe complexes

Trace a in Fig. 2 presents the spectrum of an HCOOH/Ar (1/1000) matrix in the OH stretching, C═O stretching, COH—CO

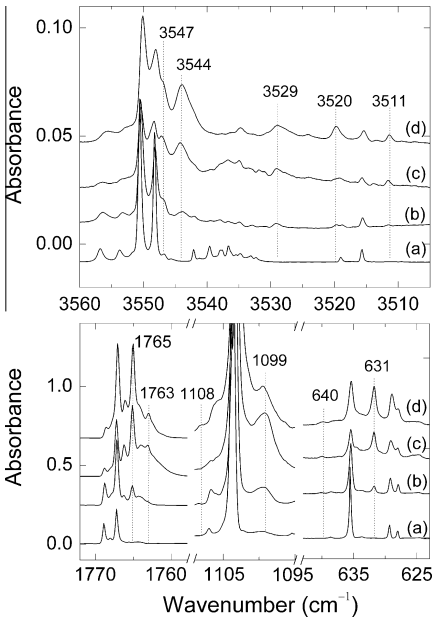

Fig. 2. FTIR spectra of (a) HCOOH/Ar = 1/1000 after deposition at 12 K; (b and c) HCOOH/Xe/Ar = 1/10/2000 after deposition at 12 and 25 K, respectively; (d) HCOOH/Xe/Ar = 1/20/2000 after deposition at 20 K.

Table 4
Characteristic frequencies and shifts (in cm^{-1}) of the FA monomers and FA···Xe complexes.

Assign.	Experiment					Calculated shift			
	Monomer[a]		Complexes			**I**	**II**	**III**	**IV**
	site 1	site 2	Freq.	Shift[b]	Assign.[c]				
cis-FA									
*ν*OH	3617.2	3615.9	3614.7	−1.8	**I**	−2.7	−22.8	−2.4	−0.8
			3613.6	−2.9	**I**				
			3591.5	−25.0	**II**				
			3589.2	−27.3	**II**				
*ν*C═O	1808.0	1806.9	1804.8	−2.6	**I**	−1.5	−4.4	−3.9	−1.9
CO—COH def	1243.4	1248.9	1251.8	+5.7	**II**	+1.5	+12.1	+1.6	+0.3
			1248.3	+2.1	**I**				
trans-FA									
*ν*OH	3550.5	3548.2	3547	−2.8	**I, III, IV**	−2.4	−26.9	−1.1	−1.2
			3544	−5.8	**I, III, IV**				
			3529	−20.	**II′**				
			3520	3	**II″**				
				−29.3					
*ν*C═O	1768.9	1767.2	1766	−2.0	**II′**	−0.7	−2.1	−2.6	−1.6
			1765	−3.0	**I, III, IV**				
			1764	−4.0	**II″**				
COH—CO def	1106.8	1106.9	1108.6	+1.7	**II″**	−0.2	+4.1	+1.1	+0.2
	1103.9	1103.6	1099.6	−4.1	**I, III, IV**				
*τ*COH	635.5	635.4	645.8	+10.3	**II″**	−1.8	+25.4	+1.2	+1.9
			640.2	+4.7	**II′**				
			631.8	−3.7	**I**				

[a] From Ref. [6].
[b] The experimental shifts are calculated with respect to the average frequencies for sites 1 and 2.
[c] **II′** and **II″** present two geometries of structure **II**.

deformation, and torsional regions measured after deposition at 12 K. In the *ν*OH region, the bands of *trans*-FA monomer (3550 and 3548 cm^{-1}) [6] and trans–trans dimers (3540 and 3537 cm^{-1}) [19] are observed after matrix deposition. The splitting of the monomer band is attributed to matrix site effects [6]. Deposition at higher temperatures (>25 K) increases the amounts of the trans–trans dimers (not shown). The experimental frequencies of the *trans*-FA species are in good agreement with the spectra reported previously, and the most characteristic bands are collected in Table 4. Co-deposition of HCOOH/Xe/Ar (1/10/2000) at 12 K results in new bands in the *ν*OH (3547, 3544, 3529, 3520, and 3511 cm^{-1}), *ν*C═O (1766, 1765, and 1763 cm^{-1}), COH—CO def (1108 and 1099 cm^{-1}), and *τ*COH (645, 640, and 631 cm^{-1}) regions (trace b). Higher deposition temperatures enhance these bands (trace c). These new absorptions are only obtained in the presence of xenon and increase in intensity with the xenon concentration (trace d), indicating that these absorptions are due to the *trans*-FA···Xe complexes. These new bands appear even at relatively low Xe concentrations; hence they are assigned to the 1:1 complexes of FA with xenon. The experimental spectra of the *trans*-FA···Xe complexes are presented in Table 4.

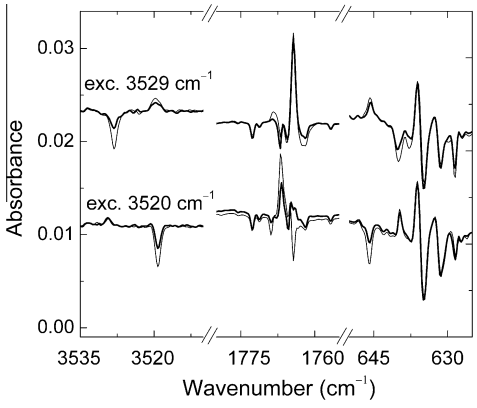

Fig. 3. Difference spectra showing the results of excitations of the H-bonded complexes (3529 and 3520 cm^{-1}) for 5 min (thick line) and 10 min (thin line). The HCOOH/Xe/Ar = 1/20/2000 matrix was deposited at 20 K.

The spectral changes obtained by selective excitation of the 3529 and 3520 cm^{-1} bands are shown in Fig. 3. For excitation at 3529 cm^{-1}, the bands at 3529, 1766, and 640 cm^{-1} bleach while the bands at 3520, 1764, 1108 and 646 cm^{-1} rise. For excitation at 3520 cm^{-1}, an opposite change takes place. The intensities of these bands are also influenced by the IR beam of the spectrometer, which decreases the intensities of the former group of bands and increases the intensities of the latter group of bands. The Xe-induced band at 3511 cm^{-1} is unchanged under broadband and selective IR excitation.

3.3. *cis*-FA···Xe complexes

In general, the vibrational excitation of *trans*-FA enhances the amount of *cis*-FA, and simultaneous annealing can lead to the formation of the *cis*-FA complexes with other matrix species. This strategy was previously used for the preparation of the *cis*-FA···H_2O [16] and *cis*-FA···N_2 [15] complexes and trans–cis FA dimers [20] with the bonded OH group. However, annealing does not enhance the amount of the *trans*-FA···Xe complexes, meaning that annealing combined with IR excitation is not an efficient strategy for the preparation of the *cis*-FA···Xe complexes. Thus, we have used another strategy. We increase the concentration of xenon and the deposition temperature to enhance the amount of the *trans*-FA···Xe complexes, and then excite the OH stretching vibrations of the *trans*-FA···Xe complexes to reorganize them to the *cis*-FA···Xe complexes. This method was used to prepare some of the trans–cis FA dimers [18,19].

Fig. 4a shows the result of excitation at 3550 cm^{-1} of the HCOOH/Xe/Ar (1/20/2000) matrix, which correspond to the OH stretching mode of *trans*-FA monomer (site 2). This excitation mainly produces the *cis*-FA monomer (site 2) with characteristic

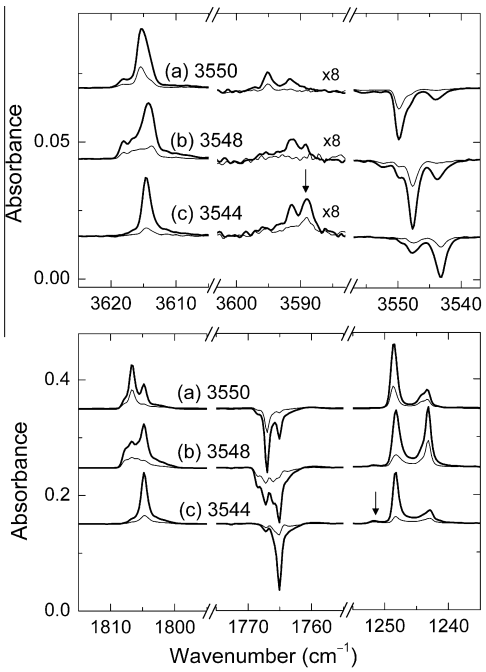

Fig. 4. Difference spectra showing the results of vibrational excitation of (a) monomer, site 2 (3550 cm^{-1}); (b) monomer, site 1 (3548 cm^{-1}); (c) complex (3544 cm^{-1}). The deposition temperature of a HCOOH/Xe/Ar = 1/20/2000 matrix is 20 K. Two weak bands of the H-bonded complex are marked by arrows. The thick and thin lines show the spectra recorded immediately after vibrational excitation and after 4 min in the dark, respectively. No long-pass filter is used in this experiment.

absorptions at 3615.9, 1806.9, and 1248.9 cm^{-1} [6]. The 3595.4 cm^{-1} band is the C=O stretching overtone of *cis*-FA. The presence of xenon leads to new bands at 3591.5 and 1804.8 cm^{-1} that are not from FA monomer. In addition, the OH stretching and deformation bands have shoulders at low-frequency sides. These new spectral features are most probably from the *cis*-FA···Xe complexes.

Fig. 4b shows the spectrum of the same sample recorded after excitation of *trans*-FA monomer at 3548 cm^{-1} (site 1). At this excitation, the depletion of *trans*-FA in site 2 becomes relatively small, and FA molecules in site 1 are efficiently pumped out as well as the Xe-induced feature at 3547 cm^{-1}. This excitation evidences the Xe-induced bands at 3614.7, 3613.6, 3591.5, 3589.2, 1804.8, and 1248.3 cm^{-1}. Also a weak band at 1251.8 cm^{-1} is observed in the deformation region.

Fig. 4c presents the result of the excitation of the *trans*-FA···Xe complex at 3544 cm^{-1}. In this case, the 3589.2 and 1251.8 cm^{-1} bands are more pronounced. The 3614.7 and 1248.3 cm^{-1} bands remain strong confirming that they are from the *cis*-FA···Xe complex. The experimental frequencies of the *cis*-FA-related species are collected in Table 4.

The *cis*-FA···Xe complexes decay with time; however, the decay rates are different (see Fig. 4). This indicates that more than one *cis*-FA···Xe structure is obtained. The bands at 3614.7, 3613.6, 1804.8 and 1248.3 cm^{-1} are less stable. The bands at 3589.2 and 1251.8 cm^{-1} are more stable. After the decay of the less stable species, weak bands at 1804 and 1801 cm^{-1} remain in the spectrum along with the 3589.2 and 1251.8 cm^{-1} bands, which probably also belong to the more stable complex. The stability of *cis*-FA monomer is between the stability of the two *cis*-FA···Xe complexes. The conversion shown in Fig. 4 is substantially accelerated during the data acquisition by the IR beam of the spectrometer.

To measure the decay rates, a long-pass filter transmitting below 1835 cm^{-1} was placed between the IR source of the spectrometer and the cryostat [4]. Fig. 5a presents the spectra of the *cis*-FA···Xe complex recorded shortly after excitation at 3544 cm^{-1} and after 6 and 15 min in the dark at 4.3 K. The bands at 1243.4, 1248.3 and 1251.8 cm^{-1} are from the CO—COH deformation mode of the *cis*-FA monomer (site 1), less stable and more stable *cis*-FA···Xe complexes, respectively. The less stable and more stable complexes are assigned to the non-H-bonded and H-bonded structures, respectively (see below). Fig. 5b compares the decays of the *cis*-FA···Xe complexes and *cis*-FA monomer obtained at 4.3 K. The lifetime of the H-bonded *cis*-FA···Xe complex is 21.5 min, which is approximately 3 and 9 times longer than the lifetimes of the *cis*-FA monomer (6.3 min) and the non-H-bonded *cis*-FA···Xe complex (2.4 min). When fitting the data for the H-bonded complex and for the monomer, the second exponent was added to account for the contribution from the short-lived non-H-bonded complex.

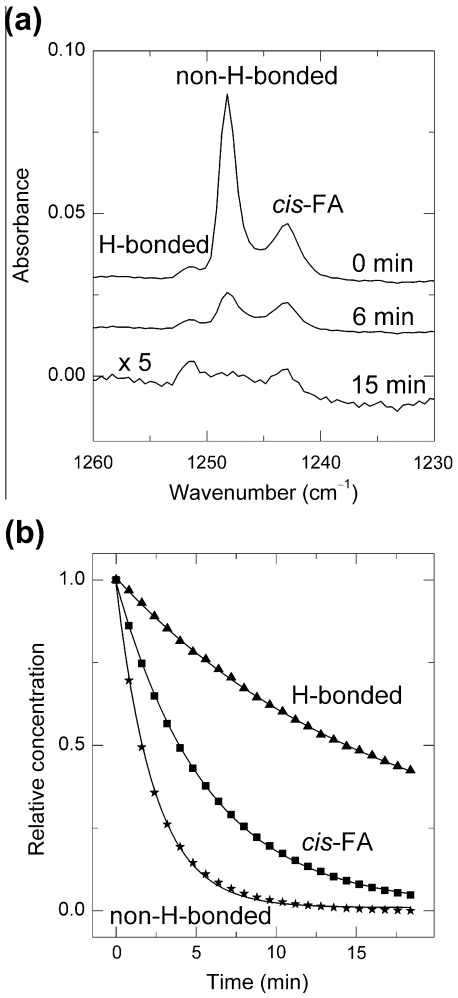

Fig. 5. Hydrogen tunnelling in *cis*-FA monomer and two *cis*-FA···Xe complexes. (a) Spectra in the CO—COH deformation region recorded at t = 0, 6, and 15 min at 4.3 K after excitation at 3544 cm^{-1}. The band at 1243.4 cm^{-1} belongs to the *cis*-FA monomer. The bands at 1248.3 and 1251.8 cm^{-1} belong to the non-H-bonded and H-bonded *cis*-FA···Xe complexes. (b) Relative concentration of these species as a function of the time at 4.3 K.

The decay rates of the *cis*-FA-related species were measured at different temperatures (Fig. 6). The lifetimes become shorter at higher temperatures, which is characteristic for the tunnelling mechanism [3,4]. At all temperatures, the decay rates are smaller for the H-bonded complex and larger for the non-H-bonded complex than those for the monomer. However, the difference of the decay rates of these species decreases at elevated temperatures.

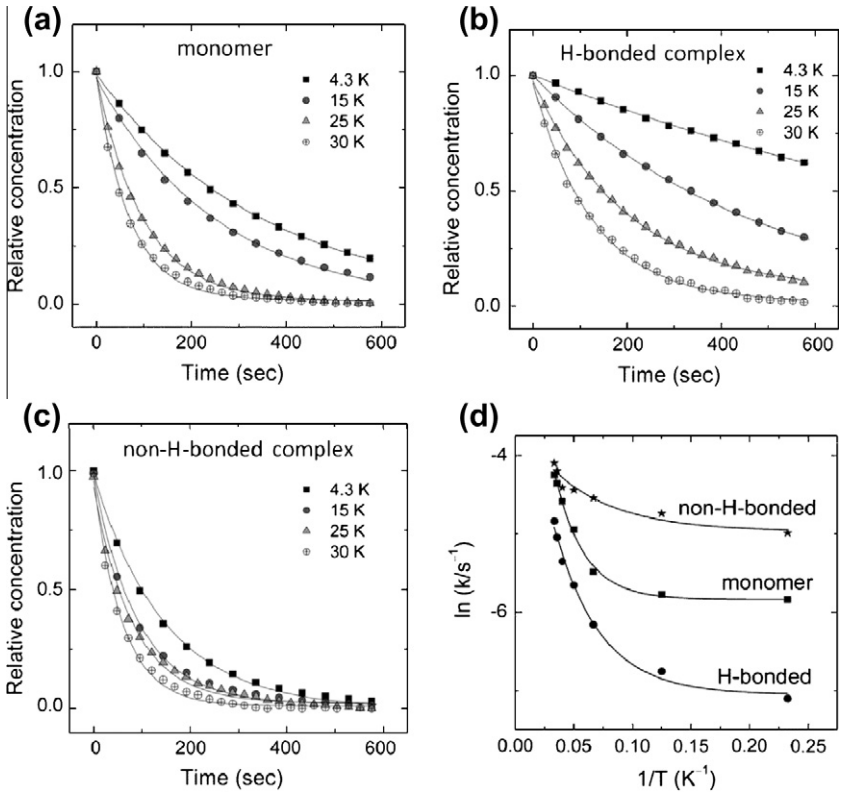

Fig. 6. (a–c) Decay of *cis*-FA monomer and *cis*-FA···Xe complexes in an argon matrix at different temperatures. (d) Decay rate constants as a function of the temperature.

For example, the lifetimes for the non-H-bonded complex, monomer, and H-bonded complex at 30 K are *ca.* 1.0, 1.1 and 2.1 min, respectively.

4. Discussion

4.1. Spectral assignment

The calculated and experimental frequency shifts for the characteristic modes of the *cis*-FA···Xe and *trans*-FA···Xe complexes are shown in Table 4. For the *trans*-FA···Xe complex, structure **II** with an OH···Xe bond is the most stable geometry. The most characteristic absorption of this complex is the OH stretching (νOH) mode, whose calculated frequency is red-shifted by $-26.9\ cm^{-1}$ from the monomer. This is in good agreement with the experimental bands at 3529 and $3520\ cm^{-1}$ with shifts of -20.3 and $-29.3\ cm^{-1}$. Under broadband IR irradiation by the Globar source at 4.3 K, the $3529\ cm^{-1}$ band decreases and the $3520\ cm^{-1}$ band increases, indicating that this configuration conversion has a small activation energy. The interconversion between these two configurations was achieved by selective vibrational excitation of the corresponding OH stretching modes (Fig. 3). The calculated shifts of the C═O stretching ($-2.1\ cm^{-1}$) and CO—COH deformation ($+4.1\ cm^{-1}$) modes of structure **II** are in good agreement with the experiments (-2.0 and $+1.7\ cm^{-1}$, respectively). The large shift ($+25.4\ cm^{-1}$) predicted for the COH torsional (τCOH) mode of structure **II** was not observed in the experiment. Based on the conversion experiments, we assign the bands at 645.8 and 640.2 cm^{-1} with shifts of +10.3 and $+4.7\ cm^{-1}$ to the H-bonded complex. The band splitting of the H-bonded complex probably originates from two similar structures with different orientations in the embedding matrix. With less probability, the band spitting originates from different matrix morphologies. Indeed, selective IR excitation did not interconvert matrix sites in the cases of FA and HONO [30,31]. The photostable band at $3511\ cm^{-1}$ may belong to the H-bonded complex in a different matrix site.

For the *trans*-FA···Xe complexes with structures **I**, **III** and **IV**, the calculations predict quite small and similar spectral changes. In experiment, these structures with non-bonded OH are consistent with the Xe-induced absorptions at 3547 and $3544\ cm^{-1}$, the averaged shift of which ($-4.3\ cm^{-1}$) agrees with the calculated values (from -1.1 to $-2.4\ cm^{-1}$). This shift is quite different from that of structure **II**. Another characteristic band is observed in the τCOH region at $631.8\ cm^{-1}$ with a shift of $-3.7\ cm^{-1}$. This red shift agrees best with the computed spectra of structure **I**, but the agreement with the calculations for structures **III** and **IV** is also acceptable. Thus, we preferably assign the group of bands at 3547, 3544, 1766, 1765, 1099.6 and $631.8\ cm^{-1}$ to structure **I**, but we cannot completely exclude at this stage structures **III** and **IV** having similar spectra. It should be emphasized that the calculations are done for the species in vacuum whereas the experiment is carried out in solid matrices, which can change the structure of the complexes. This means that more accurate calculations of the complexes in vacuum do not necessarily help discriminate these species, but one should rather model the matrix effects on the complex structures. Further complication arises from the possibility that the spectra may be contributed by interaction of FA with two and more Xe atoms; however, this contribution is supposed to be small because all main bands appear at the lowest Xe concentration.

The bands assigned to the *cis*-FA···Xe complexes are the strongest under vibrational excitation at $3544\ cm^{-1}$. The new absorptions due to *cis*-FA···Xe complex are divided into two sets: more stable and less stable. The less stable bands are observed at 3614.7, 3613.6, 1804.8 and $1248.3\ cm^{-1}$. The shifts of these bands are *ca.* $2\ cm^{-1}$ for the νOH, νC═O, and CO—COH deformation modes, which agree well with the calculations on structures **I**, **III** and **IV** of the *cis*-FA···Xe complex. The spectral shifts of these three

structures are similar to each other so that we cannot distinguish between them; however, the assignment to structure **I** is preferable. Indeed, if the *trans*-FA···Xe complex excited at 3544 cm^{-1} has structure **I**, the produced *cis*-FA···Xe complex probably has structure **I**.

The more stable bands at 3589.2 and 1251.8 cm^{-1} are assigned to structure **II** of the *cis*-FA···Xe complex, as well as the long-lived bands at 1804 and 1801 cm^{-1} heavily overlapped by the νC=O bands of the less stable complex. The shift of the OH stretching band at 3589.2 cm^{-1} is about −27 cm^{-1}, which is in good agreement with the value calculated for structure **II** (−22.8 cm^{-1}). The other band observed in this region (3591.5 cm^{-1}) decays fast under broadband IR irradiation (see Fig. 4); and it is probably from structure **II** in a different matrix site. The CO—COH def band at 1251.8 cm^{-1} is shifted by +5.7 cm^{-1} in experiment and +12.1 cm^{-1} in theory, which is also consistent with the formation of structure **II**.

4.2. Formation of the FA···Xe complexes

After deposition, the *trans*-FA···Xe complex without an OH···Xe interaction seems to be present in larger amounts compared to the H-bonded structure. This is in contrast with the calculated energies where structure **II** is slightly more strongly bound than the other structures. It is possible that the solid matrix changes the relative energies of different structures. More theoretical work is needed to understand this formation mechanism.

Two types of the *cis*-FA···Xe complex with and without OH···Xe interactions are observed. These structures are obtained upon excitation of the non-H-bonded *trans*-FA···Xe complex (3544 cm^{-1}). This is the first experimental report on the non-H-bonded *cis*-FA complex (excluding trans–cis FA dimers [18,19]). The formation of the *cis*-FA···Xe complexes without an OH···Xe interaction (structures **I**, **III**, and **IV**) may occur by rotation of the free OH group without considerable structural modification of the rest of the system. However, this simple mechanism does not work for the formation of the H-bonded structure **II**. We suggest that the H-bonded *cis*-FA···Xe complex (structure **II**) is formed by essential reorganization of the fragments in the matrix cage during vibrational energy relaxation in the *cis*-FA unit. It is worth noting that the formation of the stable *cis*-FA···Xe complex is less efficient as compared to the unstable structure; thus, this channel is minor.

4.3. Tunnelling reaction

As pointed out above**,** two types of the *cis*-FA···Xe complexes are experimentally found: H-bonded and non-H-bonded structures with slow and fast decays, respectively. The *cis*-to-*trans* decay curves and obtained decay rates for these two types of complexes at different temperatures are shown in Fig. 6. We emphasize three observations: (i) slower decay of the H-bonded complex compared to the monomer at all temperatures; (ii) faster decay of the non-H-bonded complex compared to the monomer at all temperatures; (iii) enhancement of the decay of all these species at elevated temperatures.

The decay of the *cis*-FA monomer occurs via tunnelling of the OH hydrogen atom through the torsional barrier, as discussed elsewhere [3,4,32]. The decay of the *cis*-FA···Xe complex can also be explained by this mechanism, and the barrier height is the most important factor controlling the tunnelling rate. The slower decay of the H-bonded complex can be easily explained in these terms. The *cis*-to-*trans* barrier for monomeric FA has been calculated to be 3071 cm^{-1} (ZPE-corrected 2698 cm^{-1}). In the H-bonded *cis*-FA···Xe complex (structure **II**), the interaction between the H atom of the OH group and a Xe atom lowers the total energy of the system. Hydrogen tunnelling breaks the hydrogen bond in this complex, converting the interacting system (*cis*-FA···Xe) to non-interacting system (FA + Xe pair) in the transition and final states as discussed elsewhere [15–17]. It follows that the tunnelling barrier for the H-bonded complex is higher than that for the *cis*-FA monomer approximately by the absolute value of the interaction energy. The calculations yield a stabilization barrier of 3281 cm^{-1} (ZPE-corrected 2861 cm^{-1}) for the *cis*-FA···Xe complex **II**, which is 210 cm^{-1} (ZPE-corrected 163 cm^{-1}) higher than that of the *cis*-FA monomer. In this model, the decay of the H-bonded *cis*-FA···Xe complex should be slower compared to the *cis*-FA monomer, in agreement with the experimental observations. This model has also explained the stabilization of the H-bonded *cis*-FA···N_2 and *cis*-FA···H_2O complexes [15,16]. For the *cis*-FA···N_2 complex, the decay time in an argon matrix at 9 K is about 6.5 times longer compared to that of the *cis*-FA monomer, which is consistent with a substantial increase in the stabilization barrier by 4.8 kJ mol^{-1} [15]. The stabilization barrier for the *cis*-FA···N_2 complex is also higher than that for the *cis*-FA···Xe complex (structure **II**) by 2.4 kJ mol^{-1}, which explains the longer lifetime for the nitrogen complex. Remarkably, the *cis*-FA···H_2O complex is absolutely stable at low temperatures on the scale of days, which is due to strong hydrogen bonding in this case (∼30 kJ mol^{-1}) [16].

For the non-H-bonded *cis*-FA···Xe complex, the case is different and probably more interesting. In this complex, the tunnelling H atom does not participate in the intermolecular bonding directly. Thus, as a result of hydrogen tunnelling, the interaction between FA and Xe is not efficiently affected. However, the decay of non-H-bonded complex is found to be faster than that of the monomer. This observation suggests that the stabilization barrier for this complex may be lower than that for the monomer. This is exactly what we calculated for structure **I**, which supports the assignment of the unstable bands to this specific complex (Table 3). In contrast, the stabilization barriers for structures **III** and **IV** are higher than that for the monomer, which is inconsistent with the fast decay of the unstable bands. It should be also mentioned that additional factors exist which influence the tunnelling rates [3,4,33,34].

As seen in Fig. 6d, the decay rates are enhanced by temperature for all the *cis*-FA-related species. The temperature effect is larger for the H-bonded complex compared to the monomer while it is quite small for the non-H-bonded complex. This makes the tunnelling rates of the different species more similar at elevated temperatures. The mechanism of the temperature effect on the tunnelling rate is a challenge for theoretical chemistry, which exceeds the scope of the present work.

5. Conclusions

The geometries, interaction energies, reaction barriers, and vibrational spectra of the complexes of FA and xenon have been calculated at the MP2 level of theory. Four local minima of the *trans*-FA···Xe and *cis*-FA···Xe complexes are found and the computational data are presented in Fig. 1 and Tables 1–3.

In the experiments, two types of the *trans*-FA···Xe complexes are observed after deposition of FA/Xe/Ar matrices. The spectroscopic data on the *trans*-FA···Xe complex agrees with the computational spectra of structure **II** and structure **I**, where the Xe atom is bonded to the H atom of the OH group or stacking on the carbon atom of the FA molecule, respectively. The presence of structure **III** and **IV** are not completely excluded as their spectral shifts are not much distinguishable from structure **I**.

The *cis*-FA···Xe complex is prepared by exciting the non-H-bonded *trans*-FA···Xe complex. This is the first experimental report of the non-H-bonded complex for *cis*-FA, which probably has structure **I**. The H-bonded complex (structure **II**) is also formed in small amounts. The experimental spectra of these species are in a good

agreement with the calculations. The experimental data are presented in Table 4.

The *cis*-FA···Xe complexes decay in the dark by hydrogen tunnelling. It is found that the lifetime of the H-bonded complex (structure **II**) is about 3 times longer than that of the *cis*-FA monomer at 4.3 K while the non-H-bonded complex (probably structure **I**) decays about 3 times faster than the monomer, indicating, respectively, the higher and lower stabilization barriers compared to the *cis*-FA monomer. The calculated stabilization barriers for these structures are consistent with this conclusion.

Acknowledgements

The work was supported by the Academy of Finland (Grant code 1139425) and the Finnish Centre of Excellence in Computational Molecular Science (CoE CMS). CSC – Centre for Scientific Computing Ltd. (Espoo, Finland) is acknowledged for allocated computational resources.

References

[1] W.H.Z. Hocking, Z. Naturforsch. 31A (1976) 1113.
[2] M. Pettersson, E.M.S. Maçôas, L. Khriachtchev, R. Fausto, M. Räsänen, J. Am. Chem. Soc. 125 (2003) 4058.
[3] L. Khriachtchev, J. Mol. Struct. 880 (2008) 14.
[4] M. Pettersson, E.M.S. Maçôas, L. Khriachtchev, J. Lundell, R. Fausto, M. Räsänen, J. Chem. Phys. 117 (2002) 9095.
[5] M. Pettersson, J. Lundell, L. Khriachtchev, M. Räsänen, J. Am. Chem. Soc. 119 (1997) 11715.
[6] E.M.S. Maçôas, J. Lundell, M. Pettersson, L. Khriachtchev, R. Fausto, M. Räsänen, J. Mol. Spectrosc. 219 (2003) 70.
[7] K. Marushkevich, L. Khriachtchev, J. Lundell, A.V. Domanskaya, M. Räsänen, J. Mol. Spectrosc. 259 (2010) 105.
[8] K. Marushkevich, L. Khriachtchev, M. Räsänen, J. Chem. Phys. 126 (2007) 241102.
[9] K. Marushkevich, L. Khriachtchev, M. Räsänen, Phys. Chem. Chem. Phys. 9 (2007) 5748.
[10] S. Lopes, A.V. Domanskaya, R. Fausto, M. Räsänen, L. Khriachtchev, J. Chem. Phys. 133 (2010) 144507.
[11] E.M.S. Maçôas, L. Khriachtchev, M. Pettersson, R. Fausto, M. Räsänen, J. Am. Chem. Soc. 125 (2003) 16188.
[12] E.M.S. Maçôas, L. Khriachtchev, R. Fausto, M. Räsänen, J. Phys. Chem. A 108 (2004) 3380.
[13] E.M.S. Maçôas, L. Khriachtchev, M. Pettersson, R. Fausto, M. Räsänen, J. Phys. Chem. A 109 (2005) 3617.
[14] (a) A. Olbert-Majkut, J. Ahokas, J. Lundell, M. Pettersson, Chem. Phys. Lett. 468 (2009) 176;
(b) J. Lundell, M. Räsänen, J. Phys. Chem. 97 (1993) 9657;
(c) J. Lundell, M. Räsänen, Z. Latajka, Chem. Phys. 189 (1994) 245;
(d) M. Gantenberg, M. Halupka, W. Sander, Chem. Eur. J. 6 (2000) 1865;
(e) D. Priem, T.-K. Ha, A. Bauder, J. Chem. Phys. 113 (2000) 169;
(f) W.H. Robertson, J.A. Kelley, M.A. Johnson, J. Chem. Phys. 113 (2000) 7879;
(g) L. George, E. Sanchez-Garcia, W. Sander, J. Phys. Chem. A 107 (2003) 6850.
[15] K. Marushkevich, M. Räsänen, L. Khriachtchev, J. Phys. Chem. A 114 (2010) 10584.
[16] K. Marushkevich, L. Khriachtchev, M. Räsänen, J. Phys. Chem. A 111 (2007) 2040.
[17] L. Khriachtchev, A. Domanskaya, K. Marushkevich, M. Räsänen, B. Grigorenko, A. Ermilov, N. Andrijchenko, A. Nemukhin, J. Phys. Chem. A 113 (2009) 8143.
[18] K. Marushkevich, L. Khriachtchev, J. Lundell, M. Räsänen, J. Am. Chem. Soc. 128 (2006) 12060.
[19] K. Marushkevich, L. Khriachtchev, J. Lundell, A. Domanskaya, M. Räsänen, J. Phys. Chem. A 114 (2010) 3495.
[20] K. Marushkevich, M. Siltanen, M. Räsänen, L. Halonen, L. Khriachtchev, J. Phys. Chem. Lett. 2 (2011) 695.
[21] K. Marushkevich, L. Khriachtchev, M. Räsänen, M. Melavuori, J. Lundell, J. Phys. Chem. A 116 (2012) 2101.
[22] L. Khriachtchev (Ed.), Physics and Chemistry at Low Temperatures, Pan Stanford Publishing, Singapore, 2011.
[23] I.I. Ioannou, R.L. Kuczkowski, J. Phys. Chem. 98 (1994) 2231.
[24] J. Lundell, Chem. Phys. Lett. 266 (1997) 1.
[25] P.K. Wawrzyniak, J. Panek, Z. Latajka, J. Lundell, J. Mol. Struct. 691 (2004) 115.
[26] P.K. Wawrzyniak, J. Panek, J. Lundell, Z. Latajka, J. Mol. Model. 11 (2005) 351.
[27] (a) N.P. Franks, R. Dickinson, S.L.M. de Sousa, A.C. Hall, W.R. Lieb, Nature 396 (1998) 324;
(b) R. Dickinson, B.K. Peterson, P. Banks, C. Simillis, J.C.S. Martin, C.A. Valenzuela, M. Maze, N.P. Franks, Anesthesiology 107 (2007) 756;
(c) N. Colloc'h, J. Sopkova-de Oliveira Santos, P. Retailleau, D. Vivare, F. Bonnete, B. Langlois d'Estainto, B. Gallois, A. Brisson, J.J. Risso, M. Lemaire, T. Prange, J. Abraini, Biophys. J. 92 (2007) 217.
[28] M.J. Frisch, G.W. Trucks, H.B. Schlegel, et al., Gaussian 09, Revision C.01, Gaussian, Inc., Wallingford, CT, 2010.
[29] K.A. Peterson, D. Figgen, E. Goll, H. Stoll, M. Dolg, J. Chem. Phys. 119 (2003) 11113.
[30] E.M.S. Maçôas, L. Khriachtchev, M. Pettersson, J. Juselius, R. Fausto, M. Räsänen, J. Chem. Phys. 119 (2003) 11765.
[31] L. Khriachtchev, J. Lundell, E. Isoniemi, M. Räsänen, J. Chem. Phys. 113 (2000) 4265.
[32] E.M.S. Maçôas, L. Khriachtchev, M. Pettersson, R. Fausto, M. Räsänen, Phys. Chem. Chem. Phys. 7 (2005) 743.
[33] E.M.S. Maçôas, L. Khriachtchev, M. Pettersson, R. Fausto, M. Räsänen, J. Chem. Phys. 121 (2004) 1331.
[34] A. Domanskaya, K. Marushkevich, L. Khriachtchev, M. Räsänen, J. Chem. Phys. 130 (2009) 154509.
[35] R.L. Redington, J. Mol. Spectrosc. 65 (1977) 171.